MRS Communications (2017), 7, 229–235
© Materials Research Society, 2017
doi:10.1557/mrc.2017.29

MRS Communications

Research Letter

Monitoring the adaptive cell response to hyperosmotic stress by organic devices

Pasquale D'Angelo, Giuseppe Tarabella*, Agostino Romeo**, and **Angela Giodice†**, Institute of Materials for Electronics and Magnetism, National Research Council, P.co Area delle Scienze 37/A, 43124 Parma, Italy
Simone Marasso, and **Matteo Cocuzza**, Institute of Materials for Electronics and Magnetism, National Research Council, P.co Area delle Scienze 37/A, 43124 Parma, Italy; Department of Applied Science and Technology, Politecnico di Torino, C.so Duca degli Abruzzi 24, 10129 Torino, Italy
Francesca Ravanetti, and **Antonio Cacchioli**, Department of Veterinary Sciences, University of Parma, Via del Taglio, 10, 43126 Parma, Italy
Pier Giorgio Petronini, Unit of Experimental Oncology, Department of Clinical and Experimental Medicine, University of Parma, Plesso Biotecnologico Integrato, Via Volturno, 39—Palazzina D 10 piano, 43125 Parma, Italy
Salvatore Iannotta, Institute of Materials for Electronics and Magnetism, National Research Council, P.co Area delle Scienze 37/A, 43124 Parma, Italy

Address all correspondence to Pasquale D'Angelo at **pasquale.dangelo@imem.cnr.it**

(Received 25 January 2017; accepted 25 April 2017)

Abstract

Cellular activity upon osmotic stress is related to the occurrence of several disease conditions. The real-time monitoring of the cell response to this kind of stress can give insight into the comprehension of mechanisms involved in cellular shrinkage. Currently the dynamics of the osmotic stress is studied using dedicated and tricky methodologies, not suited to the in vivo testing. We show that a disposable electronic device is very effective for studying the early stage of the osmotic stress induced on human lung adenocarcinoma cells, A549, by a hyperosmotic environment. Our findings corroborate the experimental results obtained by a standard complementary analysis.

Introduction

In the last two decades, worldwide researchers have designed and tested several types of electronic devices based on conducting polymers (CPs).[1] Some of these devices meet the demanding requirements of Organic Bioelectronics. The rise of this branch funds, in fact, on some intrinsic features of CPs, such as their mixed ionic/electronic conduction, their proven biocompatibility or their attitude to be functionalized with biomolecular side-groups, in order to impart enhanced functionalities. These features promote the CP-based thin films as the natural interface with the "biologic world",[2] hence allowing the development of analytical devices with a broad range of bioapplications such as biosensing[3,4] and the monitoring of biologic events,[5,6] or medical devices such as point of care platforms[7] and diagnostic tools.[8]

Recently, a special attention has been paid to a peculiar class of transistors, i.e., the organic electro-chemical transistors (OECTs). Although the main interest on OECTs relies on their unprecedented performances as sensors of a large variety of (bio) analytes (e.g., metallic cations,[9] micrometer-sized biomolecules,[10] DNA,[11] bacteria,[12] or marine diatoms[13]), their function covers a wide set of applications. For instance, the use of semi-biotic interfaces in OECTs architectures has allowed the implementation of multifunctional[14] and synaptic-like memory[15] devices. Currently, the use of disposable organic-based devices in the medical field as alternative tools to some standard techniques is of great relevance[2] and, in this respect, OECTs have proven to be also an effective system for the study of the cellular function and physiological activity.[16,17] In particular, OECTs integrated with a typical Transwell (Twell, a micro-porous membrane commonly used in biology as a support for cell seeding) have been successfully used for the monitoring of cellular stress.[6,18] Specifically, the barrier tissue integrity of Caco-2 cell line[6] and the effect of anticancer drugs on human lung adenocarcinoma cell line A549[18] have been tested by Twell–OECTs. In both cases, the cellular event replicated within the Twell support is monitored by the OECT in terms of a signal activated by the same event, upon opportune biasing of the gate electrode.

These works promote the Twell–OECT as a new paradigm for the study of cellular stress and the device configuration described in Ref. 18 [reported in Figs. 1(a) and 1(b)] may actually be appropriate to shed light on the features of the osmotic stress.

The failure of the adaptive cellular response to osmotic stress represents, in fact, a key issue in the study of factors associated to a wide number of human diseases. Osmotic stress is

* Current address: CAMLIN Italy Srl - Strada Budellungo 2, 43123 Parma, Italy.
** Current address: Institute for Bioengineering of Catalonia (IBEC), Baldiri Reixac, 10-12, 08028 Barcelona, Spain.
† Current address: Institute for Bioengineering of Catalonia (IBEC), C. Baldiri Reixac, 10-12, 08028 Barcelona, Spain.

https://doi.org/10.1557/mrc.2017.29 Published online by Cambridge University Press

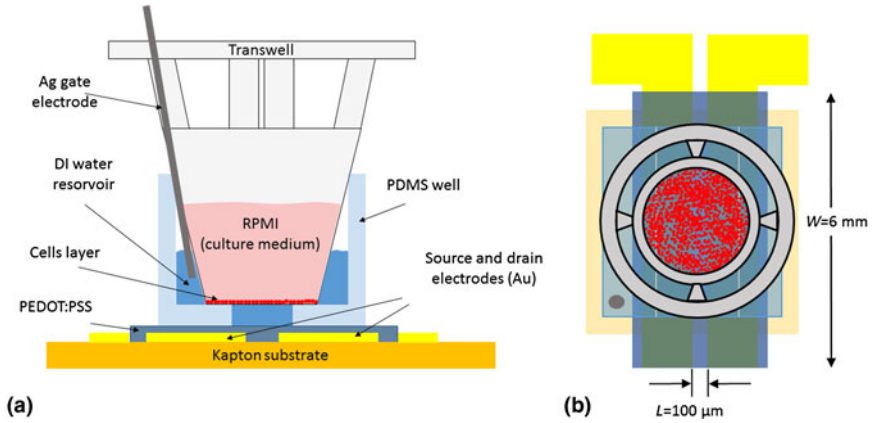


Figure 1. Front (a) and top (b) view of the device layout.

caused by an imbalance between extracellular and intracellular fluid osmolarity (both ranging between 285 and 295 mosM/kg within most tissues in normal conditions[19]). As a result, the increase in extracellular osmolarity (hyperosmosis) has many damaging effects on cells by promoting water flux out of the cell, triggering cellular shrinkage and intracellular dehydration. The loss of intracellular water adversely affects protein structure and function, provoking the alteration of the enzymatic activity. Experiments have shown that a variety of osmolytes cause, for example, release of inflammatory cytokine and inflammation.[20,21] On the other hand, osmolyte accumulation prevents water flux out of the cell, hence preserving cell volume and protecting cellular homeostasis. The hyperosmolarity of the extracellular fluid is also believed to play an inflammatory role in asthma and cystic fibrosis,[22] while a significant increase in blood glucose affects the plasma hyperosmolarity.

Several experimental techniques are used for the evaluation of the cell volume. Generally, such techniques are based on the monitoring of the intracellular concentration of internalized reagents such as fluorescent dyes (quantitative fluorescence microscopy[23,24] and radiolabeling[25]), on the use of microscopy [e.g., scanning laser confocal microscopy,[26,27] fluorescent self-quenching,[28] and scanning electron microscopy (SEM)[29]] and on electrical criterions (such as the extracellular impedance spectroscopy[25]). These techniques are often sophisticated and effective on long time scales, generally longer than those on which the dynamic evolution of the hyperosmotic shrinkage takes place. In addition, they require a dedicate equipment that, in most cases, is unsuitable to perform both an in vivo study of the cell volume variation and a dynamic analysis of the hyperosmotic stress, especially in its early stage. Conversely, Twell–OECTs turn out to be suitable for the in vitro (and in vivo) study of the dynamics of the hyperosmotic stress.[18] Hence, in this work we aim at demonstrating the working principle of a sensitive, disposable organic-based sensor for the monitoring of cellular activity in response to the hyperosmotic stress induced by the short-lasting action of non-isotonic osmolytes in the electrolyte.

Experimental

Device fabrication

OECTs have been fabricated on a 2-in. circular-shaped Kapton substrate (DuPont). The source and drain electrodes made of a Ti(20 nm)–Au(100 nm) bilayer, were deposited by using a Kurt J. Lesker PVD 75 DC Magnetron Sputtering. The Ti/Au bilayer was then patterned by a lift-off technique (image reversal AZ 5214E photoresist followed by dimethyl sulfoxide, DMSO Sigma Aldrich, bath at 60 °C), determining a 100 µm long (L) and 6 mm wide (W) device channel [Fig. 1(b)]. A mixture of PEDOT:PSS (Clevios PH1000), ethylene glycol (20:1 in volume, Sigma Aldrich) and DBSA (0.05%, Sigma Aldrich) has been spin-coated on Kapton. In this way, a 20 nm-thick film has been obtained. The spun film has been annealed at 150 °C in vacuum for 90 min. To pattern the as-prepared film, a procedure described elsewhere[30] has been followed; a 150 nm-thick Ag layer has been deposited using an ULVAC EBX-14D electron beam evaporator and subsequently patterned by a wet etching (E6 Metal Etching, 16 V H_3PO_4 (85%) : 1 V HNO_3 (65%) : 1 V CH_3COOH : 2 V H_2O) at room temperature. Finally, the PEDOT:PSS excess has been removed using a O_2 plasma (100 mTorr, 50 sccm, 100 W, 13.56 Hz) for 30 s and the residual Ag protective layer has been removed by the aforementioned E6 wet etching, defining in this way the PEDOT:PSS-based device channel. A Sylgard 184 poly(dimethylsiloxane) (PDMS, Sigma Aldrich) well with a support for the Twell (pores diameter and density 0.4 µm and 10^8 cm^{-2}, respectively; membrane area of 0.33 cm^2, Fisher Scientific Inc.) has been fabricated by soft lithography in order to confine the deionized (DI) water layer between the device channel and the bottom of the Twell.

Cell culture and counting

A549 cancer cell line (American Type Culture Collection, Manassas, VA, USA) was cultured as recommended in RPMI-1640 (Gibco LifeTechnologies) growth medium

https://doi.org/10.1557/mrc.2017.29 Published online by Cambridge University Press

supplemented with 10% fetal bovine serum (FCS), 2 mM glutamine (GLN), 1% antibiotics (penicillin 100 UI/mL, streptomycin 100 μg/mL). All cells were kept under standard cell culture conditions, at 37 °C in a water-saturated atmosphere of 5% CO_2 in air. A549 cells were then seeded in Twell supports at the densities of 5×10^4 and 10^5 cells/insert, and left to grow for 48 h in order to form a compact monolayer. Cell counting was performed by light microscopy using a Bürker hemocytometer.

Crystal violet assay, radiolabeling, and SEM

Cell vitality has been assessed by Crystal Violet [CV, triphenylmethane dye (4-[(4-dimethylaminophenyl)-phenylmethyl]-N,N-dimethyl-aniline)] assay. Cells were seeded in 12-well trays (NUNC, Rosekilde, Denmark) at a cell density of 10^5 cells per well and were exposed to an increasing osmolarity, in the range 0.3–0.7 osM, for 24 and 48 h using sucrose as conditioning osmolyte. Light excitation, which increases linearly with the cell number, was analyzed at 570 nm using a spectrophotometer. Stained cell cultures were observed by bright-field optical microscopy.

Intracellular volumes in the case of samples treated for 24 h were estimated by measuring the equilibrium distribution of 2-deoxy-D-glucose, 2-[1,2_3H(N)]. RPMI containing 5% dialyzed FCS, 2 mM GLN and 0.5 mM glucose was prepared at different osmolarity concentrations adding sucrose. Cells were incubated for 30 min at 37 °C in the presence of labeled RPMI. The radioactivity of the acid extracts was measured by scintillation counting.

In order to perform SEM, cells were treated with physiologic and 0.6 osM RPMI for 30 min and fixed with a solution of glutaraldehyde at 2,5% v/v and sodium cacodylate buffer 0.1 M (pH = 7.3) for 10 min at 4 °C. The as-prepared samples were fast dehydrated, placed on an aluminum support and covered with a thin gold–palladium layer. This protocol helps to minimize artifacts.[31] The average cell surface was quantified by sampling ≈100 cells per image for each sample (magnification: 3000×), while the cell volume decrease was estimated by calculating the intercellular free area on three different regions of a micrograph for each sample (magnification: 500×). Image analysis was performed by using the software ImageJ.

Electrical measurements

The electrical characterization of our Twell–OECTs has been carried out using a two-channel source meter (Agilent B2902) controlled by homemade LabView software, as follows. The interstice between the device channel and the bottom of the Twell has been filled with 90 μL of DI water. This content in volume ensures that the top of the DI layer is in contact with the bottom of the Twell. An Ag wire, acting as gate electrode, has been immersed in the DI water layer. Prior to start the measurement, the RPMI at a given osmolarity, ranging between 0.3 osM (control sample) and 0.6 osM, has been removed from each cultured Twell support before putting it in the PDMS well. Then, a source-to-drain voltage (V_{DS}) of −0.1 V has been applied to the channel for 20 s and, just before biasing the gate terminal (source-to-gate voltage, V_{GS}, of 0.4 V, for 210 s), the Twell support has been filled with 150 μL of physiologic RPMI. All measurements have been carried out in a cell-incubator allowing the non-isotonic osmolytes to act for 5 min prior to measure the Twell–OECT response as described just above.

Results and discussion

In the first part of this study, we have evaluated the effectiveness of the conditioning osmolyte, the sucrose, both on long time scales, where the cell shrinkage process is expected to reach an equilibrium condition, and in the early stage, where the adaptive response of cells under stress is effective.

By a CV assay, we have investigated the effect of long-lasting exposures (24 and 48 h) to the hypertonic ambient on A549 cells. The intensity of the CV coloration, proportional to the number of cells still adhered to the porous membrane of the Twell, is directly related to the cell viability upon treatment. Absorbance, evaluated by spectrophotometry [Fig. 2 (a)], shows a decrease between 0.3 and 0.6 osM, with a nearly saturating trend between 0.6 and 0.7 osM[32] that can be related

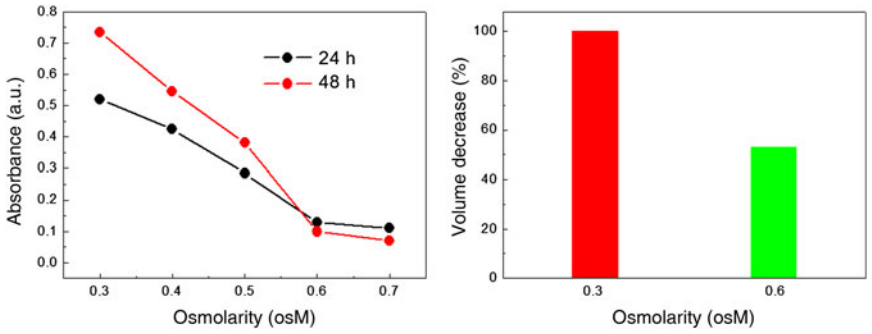


Figure 2. (a) Working osmolarity range evaluated by spectrophotometry (absorbance as a function of osmolarity); (b) cell volume assessment by radio-labeled markers for isotonic and 0.6 osM-treated samples (24 h of incubation in hypertonic ambient).

https://doi.org/10.1557/mrc.2017.29 Published online by Cambridge University Press

to the death of most of the cells exposed to a largely non-isotonic ambient.

The shrinkage of A549 cells upon 24 h-lasting incubation in a hypertonic RPMI medium (osmotic concentration 0.6 osM) has been evaluated by determining their volume variation. This has been done by assessing the concentration of labeled 2-deoxy-D-glucose in cells. Cellular shrinkage observed during 1 day of incubation to non-isotonic RPMI (at 0.6 osM), accounts for a volume reduction of 47% (Fig. 2(b)).

SEM images have been used as a complementary and efficient method to assess the effect of a non-isotonic medium on cells at the early stage of the shrinkage.[29,31] Figures 3(a) and 3(b) show micrographs of the control sample (cells in isotonic ambient) and cells exposed to 0.6 osM for 30 min, respectively. Some differences between the analyzed samples, in particular in terms of the average cell surface and intercellular gaps, are clearly evidenced by a qualitative analysis of the micrographs. For the control sample, smaller, better-adhered and interconnected cells (lower intercellular gap of about 1 μm) with respect to the case of treated cells are evidenced [see insets of Figs. 3(a) and 3(b)]. A more quantitative analysis of the micrographs has been carried out by choosing the average cell surface and the intercellular gap as the characteristic parameters of the hyperosmotic effect. As a result, the average cell surface decreased by a 43% in the treated sample with respect to the control [Fig. 3(c)], while the quantification of the intercellular gaps has shown an increase of the intercellular gap area of about 130% with respect to the control [Fig. 3(d)]. All these features are a direct consequence of the cellular shrinkage induced as a response of cells to the unbalance of osmolyte concentration in the cell culture medium. This analysis confirms the effectiveness of the cellular shrinkage on time scales of some minutes.[33]

Taking into account the above results, the cell shrinkage induced by a sucrose-enriched hypertonic ambient is investigated using a low cost and fast technology, i.e., a disposable Twell–OECT, in the range 0.3–0.6 osM (step of 0.1 osM). However, prior to checking the effect of sucrose on A549 cells, it is worth recalling the working principle of our Twell–OECT.[18]

The device configuration [Fig. 1(a)] is aimed at coupling a Twell support with the typical channel of an OECT through a dedicated PDMS well. A DI water layer fills the space separating the bottom of the Twell porous polycarbonate membrane and the transistor channel made of PEDOT:PSS. An Ag wire, acting as gate electrode, is immersed in the DI water layer. Some RPMI (rich of ionic species) is confined in the Twell, so that the underneath water layer is not directly exposed to it when the Twell membrane pores are completely clogged by a confluent layer of cells. In this case, the device response as a function of time, at fixed drain and gate voltage biasing, does not show effects ascribable to the drifting (through the membrane pores) of ions contained in the culture medium toward the underneath DI layer. Specifically, the device response is

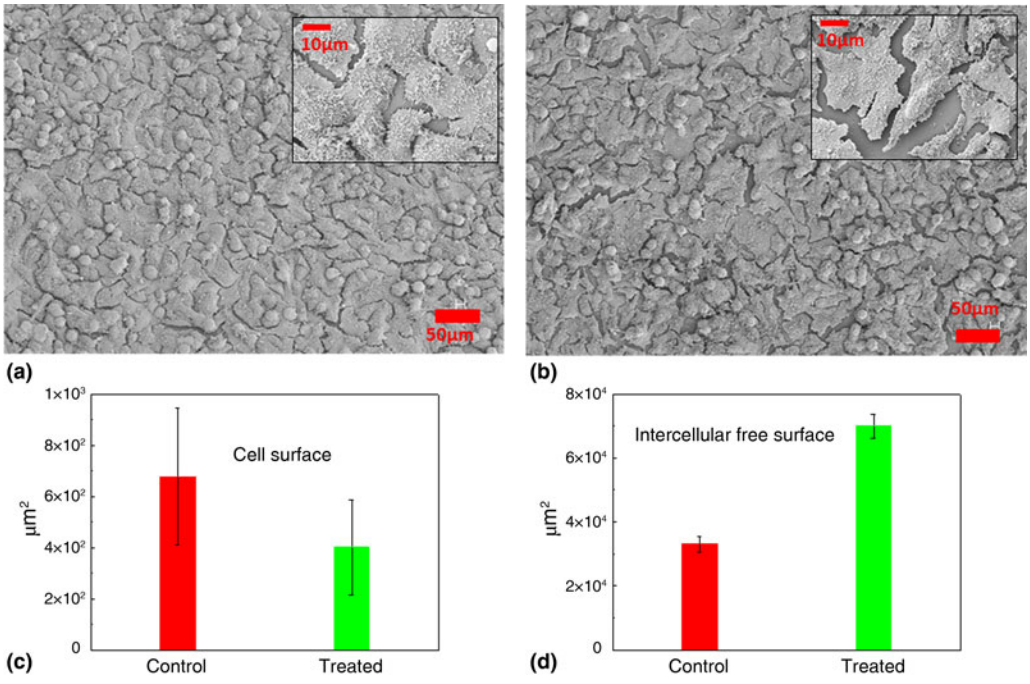


Figure 3. SEM images of (a) control and (b) 6 osM-treated cells (30 min of incubation in hypertonic ambient), cultured on Twell membranes, magnification of 500×. Insets show a magnification of 3000×; (c) average cell surface and (d) intercellular free surface calculated by image analysis of SEM micrographs for control and treated samples.

https://doi.org/10.1557/mrc.2017.29 Published online by Cambridge University Press

identical to that ascribable to an OECT operating using pure DI water as electrolyte and an Ag wire as gate electrode. Such response indicates that the confluence of the cell monolayer is preserved in an isotonic ambient. On the contrary, owing to the adaptive response of cells to the induced stress (as, for instance, the apoptotic death of cancer cells due to the effect of anticancer drugs[18]), the shielding capability of the cell layer is expected to be less effective. Hence, in this case, very small changes of the ionic population in the DI water (caused by a diffusive drift of RPMI through the exposed pores of the Twell) can be finely detected by the Twell–OECT. This detection is visualized in the form of a linear decay of the channel current as a function of time. The device response (i.e., the slope γ of the Ids versus time curve) can be modeled by using a modified Fick's law taking into account the hydraulic conductance of the Twell. The modelization provides a direct correspondence between the slope of the linear current decay and the number of pores exposed to the ionic drift (for further details, see the Supplementary Material of Ref. 18).

From the description of the device working principle, it emerges that the formation of a confluent layer of cells represents an indispensable requirement for a proper operation of our Twell–OECT. Hence, the investigation of the osmotic stress by the Twell–OECT requires a preliminary determination of the seeding conditions needed to ensure the formation of a compact layer. To this end, cells have been cultivated for 48 h on the porous membrane of the Twell at seeding densities of 5×10^4 and 10^5 cells. Then, the time-dependent OECT response ($V_{DS} = -0.1$ V) has been measured upon injection of RPMI in the Twell 30 s after the gate turning on ($V_{GS} =$ 0.4 V). Figure 4(a) shows that for the lower cell density the cell layer is not compact since ions crossing the membrane are detected by the OECT, as indicated by the I_{DS} current change that takes place about 35 s after the injection of RPMI. The observed delay of channel current decrease from the culture medium injection represents the typical drift time of the cations coming from the culture medium across the membrane pores, toward the underlying water.[18] Conversely, when the cell density realizes a complete coverage of the Twell membrane by a compact cell layer, no variation in the I_{DS} (t) signal is revealed [Fig. 4(b)], hence demonstrating that a good barrier against cations drift through the membrane is formed. Cell coverage of the Twell membrane is also showed by bright field micrographs collected upon CV staining [see insets of Figs. 4(a) and 4(b)]. Anyway, the barrier effect due to cell layer has been systematically checked for each Twell handled during the experiment. Control experiments aimed at checking the possible detection of sole sucrose by OECTs have shown that the device is insensitive to variations of the conditioning osmolyte concentration.

The effect of increasing osmotic concentrations (from 0.3 to 0.6 osM with a step of 0.1 osM) on cells treated for 5 min is showed by the time-dependent response of an OECT with a 20 nm-thick active layer [Fig. 5(a)]. It is worth to mention that we have let the non-isotonic amount of electrolyte act for 5 min prior to measure the Twell–OECT response because, as also confirmed by SEM analysis, the highest cell response to the hyperosmotic stress is expected within few minutes upon cells exposure to a non-isotonic osmolyte.[33]

Figure 5(a) shows that the device is able to reproduce unambiguously the effect of sucrose-induced stress on cells. The cell shrinkage is evidenced from the slope (γ) of the I_{ds} versus time curve, which is expected to depend on the effective number of the Twell pores exposed to the ion drift towards the DI layer, due to the shrinkage of stressed A549 cells. Even if the slope of the control sample exposed to the isotonic RPMI medium shows a deviation from the ideal case (where $\gamma = 0$ is expected), non-isotonic osmolarities determine a monotonic increase of the γ parameter in the range 0.3–0.5 osM, while the onset of a saturating trend takes place above 0.5 osM [Fig. 5(b)]. This aspect, on one hand, indicates that our device is able to detect the cell redistribution upon hyperosmotic stress, following the trend showed by CV assay even on short time scales with respect to those required for detecting the

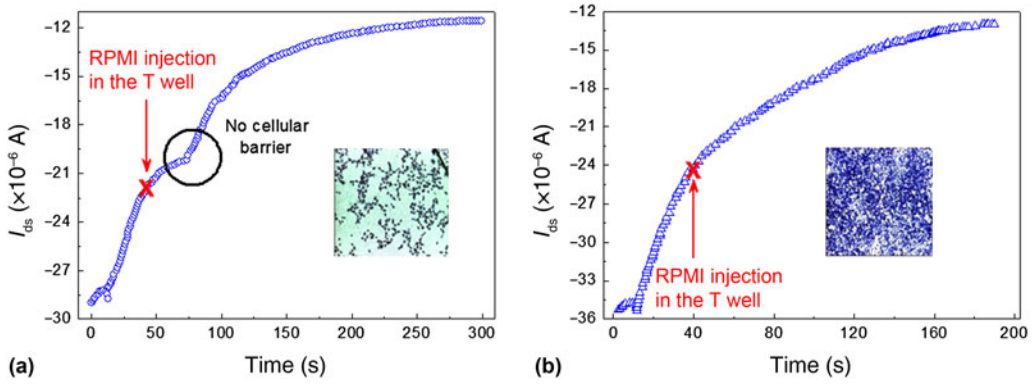


Figure 4. Seeding condition evaluated from the OECT response for cell densities of 5×10^4 (a) and 10^5 cells per Twell (b). Insets show the coverage by the cell layer of the Twell micro-porous membrane, upon coloration by CV assay.

https://doi.org/10.1557/mrc.2017.29 Published online by Cambridge University Press

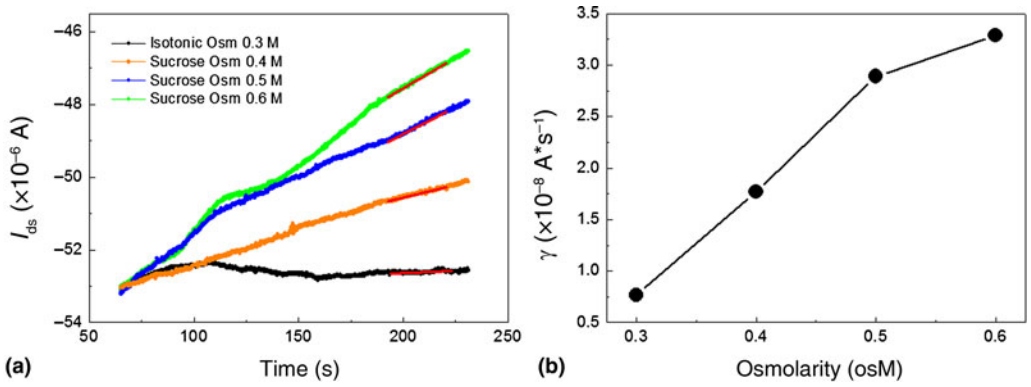


Figure 5. (a) time-dependent device response, $I_{DS}(t)$, at different osmolarities (from 0.3 to 0.6 osM); (b) γ parameter evaluated by a fitting procedure from $I_{DS}(t)$ curves.

sucrose action in this latter case. On the other hand, our results confirm that in the case of A549 cell line and sucrose as conditioning osmolyte, the most cell shrinkage upon stress takes place within few minutes of action for the non-isotonic osmolyte. In fact, taking into account the modelization of the device response,[18] the 30 min-lasting action of the 0.6 osM culture medium determines the ion drift through pores that are spread over the 44% of the Twell surface. Indeed, 24 h of exposure [Fig. 2(b)] determines a cell volume reduction of about 47% that, in terms of our model, would correspond to an exposed surface for the Twell of about 53%.

Although such analysis has regarded an exposure of 5 min to non-isotonic osmolytes, the determination of the osmotic stress dynamics during its early stage requires the assessment of the time-dependent evolution of cellular shrinkage. This can be easily done by varying the cells' exposure times to a non-isotonic solution and by mapping the distribution of γ parameters evaluated for some exposure times fixed in the desired time window.

A quite relevant aspect of this study regards the choice of a very thin PEDOT:PSS layer. This choice relies on the necessity of testing the sensitivity of Twell–OECTs when operated as amplifying stages of slow varying (and low) ionic signals. Thin channels, in fact, are reported to show a low transconductance, i.e., a low attitude at amplifying ionic signals.[34] Nevertheless, the above results indicate that the sensitivity of our device is sufficient to resolve the stress effect induced by non-isotonic osmolytes, even if it is possible to resolve subtle variations of cells volume by operating a fine tuning of the Twell–OECT sensitivity through the variation of the PEDOT:PSS thickness.

Conclusions

We show that an OECT integrated with a transwell support where A549 cells are cultivated, is a tool ideally suitable for determining the hyperosmotic stress induced by an imbalance between extracellular and intracellular fluid osmolarity. A direct evidence of a cellular shrinkage in response to the unbalance of osmolyte concentration in the cell culture medium has been found, confirming the effectiveness of sucrose as conditioning electrolyte even on time scales shorter than those required by the complementary analysis carried out in this work (CV assay, radiolabeling, and SEM). Our results pave the way for a real-time investigation of both the early stage and the dynamics of cell shrinkage upon hyperosmotic stress and, more in general, for the study of mechanisms involved in cells activity.

Acknowledgments

This work has been funded by the N-Chem project within the CNR–NANOMAX Flagship program, by the Provincia Autonoma di Trento, call "Grandi progetti 2012", project "Madelena" and by "NANONOPAIN-Theras" project co-funded by POR-FESR 2014-2020, Regione Emilia Romagna.

References

1. T.K. Das and S. Prusty: Review on conducting polymers and their applications. *Polym. Plast. Technol. Eng.* **51**, 1487 (2012).
2. R.M. Owens and G.G. Malliaras: Organic Electronics at the Interface with Biology. *MRS Bull.* **35**, 449 (2010).
3. S. Nambiar and J.T.W. Yeow: Conductive polymer-based sensors for biomedical applications. *Biosens. Bioelectron.* **26**, 1825 (2011).
4. I. Cesarino, H.V. Galesco, F.C. Moraes, M.R.V. Lanza, and S.A.S. Machado: Biosensor based on electrocodeposition of carbon nanotubes/polypyrrole/laccase for neurotransmitter detection. *Electroanalysis* **25**, 394 (2013).
5. G. Tarabella, A. Pezzella, A. Romeo, P. D'Angelo, N. Coppedè, M. Calicchio, M. D'Ischia, R. Mosca, and S. Iannotta: Irreversible evolution of eumelanin redox states detected by an organic electrochemical transistor: en route to bioelectronics and biosensing. *J. Mater. Chem. B* **1**, 3843 (2013).
6. L.H. Jimison, S.A. Tria, D. Khodagholy, M. Gurfinkel, E. Lanzarini, A. Hama, G.G. Malliaras, and R.M. Owens: Measurement of barrier tissue integrity with an organic electrochemical transistor. *Adv. Mater.* **24**, 5919 (2012).
7. D. Svirskis, J. Travas-Sejdic, A. Rodgers, and S. Garg: Electrochemically controlled drug delivery based on intrinsically conducting polymers. *J. Control. Release* **146**, 6 (2010).

https://doi.org/10.1557/mrc.2017.29 Published online by Cambridge University Press

8. F. Cicoira and C. Santato: *Organic Electronics: Emerging Concepts and Technologies*, 1st ed. (Verlag GmbH & Co. KGaA: Weinheim, Germany, 2013), pp. 69–89.
9. P.-O. Svensson, D. Nilsson, R. Forchheimer, and M. Berggren: A sensor circuit using reference-based conductance switching in organic electrochemical transistors. *Appl. Phys. Lett.* **93**, 203301 (2008).
10. G. Tarabella, A.G. Balducci, N. Coppedè, S. Marasso, P. D'Angelo, S. Barbieri, M. Cocuzza, P. Colombo, F. Sonvico, R. Mosca, and S. Iannotta: Liposome sensing and monitoring by organic electrochemical transistors integrated in microfluidics. *Biochim. Biophys. Acta—Gen. Subj.* **1830**, 4374 (2013).
11. P. Lin, X. Luo, I.M. Hsing, and F. Yan: Organic electrochemical transistors integrated in flexible microfluidic systems and used for label-free DNA sensing. *Adv. Mater.* **23**, 4035 (2011).
12. R.-X. He, M. Zhang, F. Tan, P.H.M. Leung, X.-Z. Zhao, H.L.W. Chan, M. Yang, and F. Yan: Detection of bacteria with organic electrochemical transistors. *J. Mater. Chem.* **22**, 22072 (2012).
13. J. Liao, S. Lin, K. Liu, Y. Yang, R. Zhang, W. Du, and X. Li: Organic electrochemical transistor based biosensor for detecting marine diatoms in seawater medium. *Sens. Actuators B, Chem.* **203**, 677 (2014).
14. G. Tarabella, P. D'Angelo, A. Cifarelli, A. Dimonte, A. Romeo, T. Berzina, V. Erokhin, and S. Iannotta: A hybrid living/organic electrochemical transistor based on the *Physarum polycephalum* cell endowed with both sensing and memristive properties. *Chem. Sci.* **6**, 2859 (2015).
15. A. Romeo, A. Dimonte, G. Tarabella, P. D'Angelo, V. Erokhin, and S. Iannotta: A bio-inspired memory device based on interfacing *Physarum polycephalum* with an organic semiconductor. *APL Mater.* **3**, 014909 (2015).
16. C. Yao, C. Xie, P. Lin, F. Yan, P. Huang, and I.M. Hsing: Organic electrochemical transistor array for recording transepithelial ion transport of human airway epithelial cells. *Adv. Mater.* **25**, 6575 (2013).
17. P. Lin, F. Yan, J. Yu, H.L.W. Chan, and M. Yang: The application of organic electrochemical transistors in cell-based biosensors. *Adv. Mater.* **22**, 3655 (2010).
18. A. Romeo, G. Tarabella, P. D'Angelo, C. Caffarra, D. Cretella, R. Alfieri, P. G. Petronini, and S. Iannotta: Drug-induced cellular death dynamics monitored by a highly sensitive organic electrochemical system. *Biosens. Bioelectron.* **68**, 791 (2015).
19. J.G. Verbalis: Disorders of body water homeostasis. *Best Pract. Res. Clin. Endocrinol. Metab.* **17**, 471 (2003).
20. H. Kim, J.Y. Seo, and K.H. Kim: Effects of mannitol and dimethylthiourea on Helicobacter pylori-induced IL-8 production in gastric epithelial cells. *Pharmacology* **59**, 201 (1999).
21. J.G.S. Gong Wei, Q. Huang, J. Li, Z. Liu, H. You, and Y. Chen: Taurine attenuates liver injury by downregulating phosphorylated p38 MAPK of Kupffer cells in rats with severe acute pancreatitis. *Inflammation* **35**, 690 (2012).
22. W. Neuhofer: Role of NFAT5 in inflammatory disorders associated with osmotic stress. *Curr. Genomics* **11**, 584 (2010).
23. G.M. Lee: Measurement of volume injected into individual cells by quantitative fluorescence microscopy. *J. Cell Sci.* **94**, 443 (1989).
24. W. Crowe, J. Altamirano, L. Huerto, and F. Alvarez-Leefmans: Volume changes in single N1E-115 neuroblastoma cells measured with a fluorescent probe. *Neuroscience* **69**, 283 (1995).
25. H.K. Kimelberg, E.R. O'Connor, P. Sankar, and C. Keese: Methods for determination of cell volume in tissue culture. *Can. J. Physiol. Pharmacol.* **70**(Suppl.), S323 (1992).
26. F. GUILAK: Volume and surface area measurement of viable chondrocytes in situ using geometric modelling of serial confocal sections. *J. Microsc.* **173**, 245 (1994).
27. Y.E. Korchev, M. Milovanovic, C.L. Bashford, D.C. Bennett, E. V. Sviderskaya, I. Vodyanoy, and M.J. Lab: Specialized scanning ion-conductance microscope for imaging of living cells. *J. Microsc.* **188** (Pt 1), 17 (1997).
28. S. Hamann, J.F. Kiilgaard, T. Litman, F.J. Alvarez-Leefmans, B.R. Winther, and T. Zeuthen: Measurement of cell volume changes by fluorescence self-quenching. *J. Fluoresc.* **12**, 139 (2002).
29. A.S.G. Curtis: Cell reactions with biomaterials: the microscopies. *Eur. Cells Mater.* **1**, 59 (2001).
30. S. Ouyang, Y. Xie, D. Zhu, X. Xu, D. Wang, T. Tan, and H.H. Fong: Photolithographic patterning of PEDOT:PSS with a silver interlayer and its application in organic light emitting diodes. *Org. Electron.* **15**, 1822 (2014).
31. A. Katsen-Globa, N. Puetz, M.M. Gepp, J.C. Neubauer, and H. Zimmermann: Study of SEM preparation artefacts with correlative microscopy: cell shrinkage of adherent cells by HMDS-drying. *Scanning* **38**, 625 (2016).
32. S. La Monica, C. Caffarra, F. Saccani, E. Galvani, M. Galetti, C. Fumarola, M. Bonelli, A. Cavazzoni, D. Cretella, R. Sirangelo, R. Gatti, M. Tiseo, A. Ardizzoni, E. Giovannetti, P.G. Petronini, and R.R. Alfieri: Gefitinib inhibits invasive phenotype and epithelial-mesenchymal transition in drug-resistant NSCLC cells with MET amplification. *PLoS ONE* **8**, e78656 (2013).
33. T.R. Kiehl, D. Shen, S.F. Khattak, Z. Jian Li, and S.T. Sharfstein: Observations of cell size dynamics under osmotic stress. *Cytometry A* **79 A**, 560 (2011).
34. D. Khodagholy, J. Rivnay, M. Sessolo, M. Gurfinkel, P. Leleux, L. H. Jimison, E. Stavrinidou, T. Herve, S. Sanaur, R.M. Owens, and G. G. Malliaras: High transconductance organic electrochemical transistors. *Nat. Commun.* **4**, 2133 (2013).

https://doi.org/10.1557/mrc.2017.29 Published online by Cambridge University Press